DOI: 10.1021/ma101348k

Macromolecules
ARTICLE

Polystyrene-*block*-poly(*n*-butyl acrylate)-*block*-polystyrene Triblock Copolymer Thermoplastic Elastomer Synthesized via RAFT Emulsion Polymerization

Yingwu Luo,*,† Xiaoguang Wang,† Yue Zhu,† Bo-Geng Li,*,† and Shiping Zhu*,‡

†*The State Key Laboratory of Chemical Engineering, Department of Chemical and Biochemical Engineering, Zhejiang University, 38 Zhe Da Road, Hangzhou 310027, PR China, and* ‡*Department of Chemical Engineering, McMaster University, Hamilton, Ontario L8S 4L7, Canada*

Received June 20, 2010; Revised Manuscript Received August 3, 2010

ABSTRACT: A series of well-controlled polystyrene-*b*-poly(*n*-butyl acrylate)-*b*-polystyrene triblock copolymers were prepared by emulsion polymerization with a carefully designed amphiphilic macroRAFT (reversible addition−fragmentation chain transfer) agent. The triblock copolymers were produced within four hours and only a few percent of dead chains were estimated. Tensile strength of the materials was a function of composition only and it increased linearly with polystyrene composition up to 50 wt %. The ultimate tensile strength reached 10 MPa with an elongation at break of 500% at the polystyrene composition of 40−50 wt %.

Introduction

Polystyrene-*b*-polybutadiene-*b*-polystyrene triblock copolymers (SBS) has been widely used as thermoplastic elastomer (TPE), which combines the mechanical performance of vulcanized rubbers and the energy-saving processing and recyclable nature of thermoplastics. The unique thermomechanical properties of TPEs are associated with the phase morphology of "hard" plastic nanodomains dispersed in a continuous rubbery matrix. Living polymerization is a straightforward method for the preparation of these multiblock copolymers. In industry, SBS and polystyrene-*b*-polyisoprene-*b*-polystyrene (SIS) are synthesized by living anionic polymerization. However, anionic polymerization is very intolerant to functionality and impurities, requiring low temperature, rigorous purification of reagents and exhausting removal of moisture. It remains a great challenge to synthesize polar triblock copolymers directly from vinyl monomers via anionic polymerization. As a matter of fact, poly(methyl methacrylate)(PMMA)-*b*-poly(alkyl acrylate)-*b*-PMMA were only synthesized by transesterification of *tert*-butyl ester groups of PMMA-*b*-poly(*t*-butyl acrylate)-*b*-PMMA precursors.[1−3]

On the other hand, controlled/living radical polymerizations (CLRP) have been investigated extensively over the past decades because these methods are versatile with almost all types of vinyl monomers and with emulsion and suspension polymerization processes where water is used as polymerization media.[4] The three best known CLRP techniques are NMP (nitroxide mediated polymerization),[5] ATRP (atom transfer radical polymerization),[6,7] and RAFT (reversible addition−fragmentation chain transfer radical polymerization).[8] Polystyrene-*b*-poly(*n*-butyl acrylate)-*b*-polystyrene (PSt−PnBA−PSt) triblock copolymers were synthesized via two-step bulk NMP by Gnanou et al.[9] and two-step bulk RAFT by Mayadunne et al.[10] The final copolymer had a molecular weight over 100 kg/mol. Jerome et al. synthesized PMMA-*b*-poly(*n*-butyl acrylate)-*b*-PMMA (PMMA−PnBA−PMMA) copolymers by two-step bulk-solution ATRP.[11−13] Matyjaszewski et al.[14−16] synthesized PMMA-*b*-poly(*t*-butyl acrylate)-*b*-PMMA and polystyrene-*b*-poly(*t*-butyl acrylate)-*b*-polystyrene of Mn < 100 kg/mol via bulk and solution ATRP. In general, it often takes tens of hours to prepare triblock copolymers by CLRP in solution and bulk, due to the very low radical concentrations.[17] The radical concentration is reduced to a very low level on purpose to suppress the irreversible termination, which is essential for a high molecular weight product, as required by triblock copolymer thermoplastic elastomers.

The mechanical properties of triblock copolymers synthesized from CLRP are scarcely investigated. Jerome et al. reported that the ATRP triblock PMMA−PnBA−PMMA had much poorer ultimate tensile strength and elongation at break than its anionic polymerization counterpart.[2] For example, their best results were 5.0 MPa with 385% in ref 11 and 4.2 MPa with 415% in ref 12, even though the copolymers had PDIs as low as 1.18 and 1.15, respectively. The authors hypothesized that the poor mechanical properties be ascribed to the relatively broad molecular weight distribution of the PMMA blocks. In addition, it was concluded that a small fraction of diblock copolymer could dramatically deteriorate the mechanical properties of the triblock copolymer.[18] It is likely that a small fraction of PMMA-*b*-PnBA diblock was present in the reported PMMA−PnBA−PMMA product.[11,12]

It has been recognized that RAFT (mini)emulsion polymerization has certain advantages in synthesizing triblock copolymer elastomers. Compared to homogeneous systems, the heterogeneous (mini)emulsion facilitates suppression of irreversible radical termination and shortens the polymerization time through a radical segregation effect.[19−25] However, RAFT (mini)emulsion polymerization is a very complicated process. A decade of extensive investigations has provided some insight and understanding.[4] For example, superswelling of oligomer particles generated at an early stage has become an accepted explanation for colloidal instability, loss of control in molecular weight, broadening of molecular weight distribution and particle size distribution, which are often observed in RAFT miniemulsion and ab initio emulsion polymerization.[26,27] RAFT (mini)emulsion polymerization rate could be retarded by a low nucleation efficiency[20,28]

*Corresponding authors.

 Published on Web 08/17/2010

and the RAFT reaction equilibrium.[29−31] So far, well-controlled RAFT miniemulsion polymerizations of styrene,[19,28,32−43] butyl acrylate,[38,44] methyl methacrylate,[19,35,36,39−41,45] and vinyl acetate[46,47] have been achieved by increasing surfactant and costabilizer levels,[32−43,46,47] careful selection of RAFT agents,[19,28,38,44] and optimization of polymerization temperature.[19,45] The RAFT ab initio emulsion polymerization of styrene and *n*-butyl acrylate could be successfully carried out using carefully designed amphiphilic macroRAFT agent as both chain transfer agent and surfactant.[48−53]

To our best knowledge, there are only a few papers reporting synthesis of triblock copolymers via heterogeneous CLRP. PSt−PnBA−PSt triblock copolymer was synthesized via two-step NMP emulsion polymerization.[54−56] The reaction lasted about 14 h and the final product had a molecular weight of Mn < 60 kg/mol. The RAFT miniemulsion polymerization was applied to synthesize PSt−PnBA−PSt using difunctional RAFT agent.[38] The M_n's of the triblock copolymers deviated significantly from their theoretical values and their molecular weight distributions (PDIs) were also broad. There were no mechanical property data reported for these polymers.

Very recently, our group found that when a block co-oligomer of poly(acrylic acid)$_{27}$-*b*-polystyrene$_5$ ($PAA_{27}-PSt_5$) trithiocarbonate macroRAFT agent was used as a surfactant, an excellent control over styrene RAFT emulsion polymerization could be achieved.[57] When the RAFT agent was not neutralized at the nucleation stage, the polymerization had a high rate, yielded a predicted molecular weight and narrow molecular weight distribution, and contained little coagulum. In this study, the developed technique is used to synthesize a series of polystyrene-*b*-poly(*n*-butyl acrylate)-*b*-polystyrene (PSt−PnBA−PSt) triblock copolymers with few dead chains. The mechanical properties of the PSt−PnBA−PSt triblock copolymers can thus be systematically investigated for the first time.

Experimental Part

Materials. Acrylic acid and styrene were distilled under reduced pressure prior to emulsion polymerization. *n*-Butyl acrylate (nBA) was washed with sodium hydroxide aqueous solution (5 wt %) to remove the inhibitor. Potassium persulfate (KPS, >99%), 4,4′-azobis-(4-cyanopentanoic acid) (V501, >99%), 1,4-dioxane (>99%) and sodium hydroxide (NaOH, >96%) were directly used without further purification. The small RAFT agent, 2-(((dodecylsulfanyl) carbonothioyl) sulfanyl) propanoic acid, was synthesized and purified as described in ref 48.

Synthesis of Poly(acrylic acid)$_{28}$-*b*-polystyrene$_5$ Trithiocarbonate MacroRAFT Agent. The PAA−PSt macroRAFT agent was synthesized by a two-step solution polymerization. First, a solution containing 1.5 g (4.3×10^{-3} mol) of the small RAFT agent, 0.12 g (4.3×10^{-4} mol) of V501, 9.3 g (0.13 mol) of acrylic acid, and 25 g of dioxane were introduced to a flask, and the reaction proceeded with stirring at 80 °C for 6 h. The flask was then cooled down to room temperature and another solution containing 4.5 g (4.3×10^{-2} mol) of styrene, 0.12 g (4.3×10^{-4} mol) of V501, and 5 g of dioxane was added. The mixture was deoxygenated and reacted for a further 12 h at 80 °C. The product (macroRAFT agent) was collected by precipitation of the mixture in cyclohexane. The macroRAFT agent was dried under vacuum at 50 °C. The yield of $PAA_{28}-PSt_5$ macroRAFT agent was 80%, estimated by gravimetric analysis and ^{1}H NMR.

Synthesis of PSt−PnBA−PSt Triblock Copolymer via Emulsion Polymerization Mediated by $PAA_{28}-PSt_5$ Trithiocarbonate MacroRAFT Agent. Taking experiment 1 as an example (as shown in Scheme 1), 0.63 g (2.3×10^{-4} mol) of the macroRAFT agent was dissolved in 40 g of deionized water without neutralization and the aqueous pH value was about 2.8. Then 7 g (6.7×10^{-2} mol) of styrene was mixed with the aqueous solution in a 100 mL flask. During 30 min deoxygenation by nitrogen purge, the temperature was increased to 70 °C. The initiator potassium persulfate (KPS, 0.012 g, 4.4×10^{-5} mol, in 3.0 g deionized water) was injected to start the emulsion polymerization. After 70 min, 0.90 g (2.2×10^{-2} mol, in 3 g deionized water) NaOH was injected and the second monomer 6.0 g (4.7×10^{-2} mol) of *n*-butyl acrylate was added at 20 g/h. The polymerization of *n*-butyl acrylate proceeded for 50 min (including the addition of the monomer). After that, the third monomer 7.0 g (6.7×10^{-2} mol) of styrene was added at 20 g/h. The polymerization of styrene lasted 85 min (including the feeding period) and the reaction was then completed. Samples were withdrawn during the process for gravimetric, GPC, and Malvern ZETASIZER analysis.

Scheme 1. Synthesis Route of Polystyrene-*b*-poly(*n*-butyl acrylate)-*b*-polystyrene (PSt−PnBA−PSt) Triblock Copolymer via Emulsion Polymerization Mediated by Poly(acrylic acid)$_{28}$-*b*-polystyrene$_5$ ($PAA_{28}-PSt_5$) MacroRAFT Agent

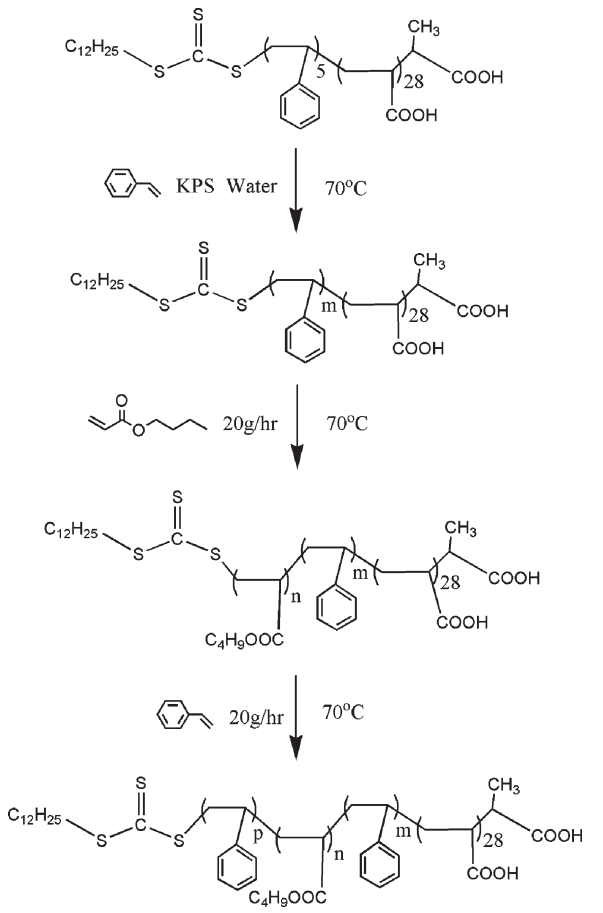

NMR Analysis. The structure of the macroRAFT agent was determined by ^{1}H NMR using DMSO as solvent on a BRUKER DMX 500 MHz spectrometer. ^{1}H NMR signals of $PAA_{28}-PSt_5$ macroRAFT agent were assigned as follows (in ppm): 0.84 (3H, $-CH_3$ of $-C_{12}H_{25}$ chain moiety), 1.04 (3H, $-CH_3$ of $-CHCH_3$-(COOH) chain moiety), 1.24 (18H, $-CH_2(CH_2)_9CH_3$ of $-C_{12}H_{25}$ chain), 1.52 ($-C-CH_2-C-$ of PAA−PSt chain), 2.21 (−CH-(COOH) − of PAA chain), 7.13 (25H, −Ph−H of PSt chain), 12.2 (29H, −COOH of PAA chain), 1.75, 3.57 (H of impurities dioxane). The signal at 0.86 ppm (3H, $-CH_3$ of $-C_{12}H_{25}$ chain moiety) was used to estimate the composition. The PAA_{28}-PSt_5 macroRAFT agent contains 28 acrylic acid units (12.2 ppm, 29 H, contain one H from the small RAFT agent) and 5 styrene units (7.13 ppm, 25 H). The M_n by ^{1}H NMR is 2886 g/mol. The composition of PSt−PnBA−PSt triblock copolymers was determined by ^{1}H NMR using $CDCl_3$ as solvent.

GPC Analysis. Molecular weights and PDIs were measured by GPC (Waters 1525 Binary HPLC Pump, Waters 2414 Refractive Index Detector, Waters 717 Autosampler). UV 311 signals were detected by Waters 2487 Dual λ Absorbance Detector. The samples were dried in a vacuum oven at 120 °C for 2 h and then dissolved in tetrahydrofuran (THF) which contained 2 wt % 1 M hydrochloric acid aqueous solution to mask COOH group interactions with GPC columns.[58] The eluent was THF with a flow rate of 1.0 mL/min and the testing temperature was 30 °C. Considering the different molecular weights, two sets of Waters Styragel columns (HR 5, 4, 3 (the measured range: 4 000 000−500 g/mol) and HR 4, 3, 1 (the measured range: 500 000−100 g/mol)) were utilized. The molecular weights and PDIs were derived from a calibration curve based on narrow polystyrene standards.

Particle Size Analysis. The particle size and distribution were measured by Malvern ZETASIZER 3000 HAS at 25 °C. The samples were dried in vacuum at 30 °C for 2 h to remove residual monomer. The number of particles (N_p), was calculated by

$$N_p = \frac{6m}{\pi {D_v}^3 d_p}$$

where m is the polymer mass in grams ($g_{\text{latex}}{}^{-1}$), d_p is the polymer density 1.05 g·cm^{-3}, and D_v is the volume-average particle diameter measured by Malvern.

Sample Preparation. For tensile measurements, the films were prepared by casting a copolymer solution in THF (10 wt %). The solvent was evaporated over 3 days at room temperature. The films were dried to constant weight in a vacuum oven at 120 °C for 24 h.

Hardness Measurement. The Shore A hardness (H_A) was measured by LX-A Shore Rubber Hardness. The test method is GB 2411−80. Each hardness measurement was repeated at least 5 times.

Tensile Tests. The mechanical properties were measured by Zwick/Roell Z020 universal material tester. The test method is GB 16421−1996. The testing samples were cut from the solution cast films and extended at 50 mm/min at room temperature. Each measurement was repeated at least four times.

pH Value Measurement. The initial pH value of the aqueous phase was measured by LEICI PHS-2C pH-meter. The electrode type was E201−4.

DSC Analysis. Differential scanning calorimetry (DSC) was carried out with a TA Q200 instrument. The heating rate was 10 °C/min. The glass transition temperature (T_g) was reported at the inflection point of the heat capacity jump.

TEM Observations. The transmission electron microscopy (JEOL JEMACRO-1230) was used to observe the phase morphology of PSt−PnBA−PSt triblock sample at the operating voltage of 80 kV. The polystyrene block of the samples was selectively stained by RuO_4.[59]

Results and Discussion

Synthesis of PSt−PnBA−PSt Triblock Copolymer via RAFT Emulsion Polymerization. For triblock thermoplastic elastomers, it is generally accepted that if the molecular weight of the "hard" block is higher than its entanglement molecular weight (M_e), the copolymer composition becomes the major chain structure parameter in determining TPE's mechanical properties.[60] To investigate these factors, three sets of experiment were designed, as shown in Table 1. Experiments 1−7 were designed to have the same PSt block molecular weight (ca. 30K g/mol) and the copolymer composition was varied by changing poly(*n*-butyl acrylate)(PnBA) block length from 25 to 240 kg/mol. For the SBS products made from anionic polymerization, it is known that PSt M_n of 15 kg/mol is adequate for high tensile strength. Considering that the higher PDI's of PSt block by the RAFT

Table 1. Synthesis of PSt−PnBA−PSt Triblock Copolymer via Emulsion Polymerization Mediated by PAA_{28}-PSt_5 MacroRAFT Agent

			polystyrene				PSt−PnBA diblock copolymer				PSt−PnBA−PSt triblock copolymer			
exp[a]	sample[b]	$M_{n,exp,PSt-PnBA-PSt}$[c]	convn[d] (%)	t (min)	$M_{n,th}$[e] (g/mol)	$M_{n,exp}$ (g/mol)	PDI	convn[d] (%)	t (min)	$M_{n,th}$[e] (g/mol)	$M_{n,exp}$ (g/mol)	PDI	convn[d] (%)	t (min)	$M_{n,th}$[e] (g/mol)	$M_{n,exp}$ (g/mol)	PDI
1	30K−25K−30K	33K−22K−31K	95	70	31 800	32 700	1.25	92	50	54 400	54 700	1.37	95	85	84 600	86 100	1.41
2	30K−55K−30K	36K−53K−23K	98	70	32 800	36 000	1.25	94	60	87,400	89,000	1.46	92	85	112 200	112 300	1.63
3	30K−70K−30K	33K−67K−31K	92	70	31 000	33 300	1.35	95	65	99 700	100 000	1.64	96	60	130 600	131 300	2.36
4	30K−90K−30K	32K−89K−28K	90	75	30 900	31 800	1.37	98	80	119 600	120 800	2.53	97	55	148 400	149 100	2.41
5	30K−110K−30K	34K−110K−25K	95	75	32 000	34 000	1.36	97	75	138 700	143 700	2.23	95	55	164 400	169 000	2.67
6	30K−140K−30K	34K−138K−29K	96	75	32 700	34 400	1.37	95	85	168 300	172 300	2.88	96	55	197 800	201 000	2.99
7	30K−240K−30K	38K−270K−23K	99	75	33 900	37 800	1.42	98	85	275 000	314 700	3.02	96	50	303 500	338 100	3.19
8	15K−90K−15K	16K−86K−14K	95	60	16 600	16 500	1.34	93	85	100 500	102 100	1.96	90	60	110 700	115 800	1.94
9	45K−90K−45K	47K−96K−50K	99	100	47 100	47 500	1.35	97	70	135 600	144 100	2.16	96	70	182 400	195 000	2.29
10	15K−45K−15K	18K−44K−15K	98	60	17 600	18 200	1.40	95	70	59 900	61 800	2.02	95	60	74 100	76 800	2.01
11	45K−135K−45K	48K−132K−38K	99	100	47 300	47 600	1.37	98	85	179 300	189 300	2.69	96	55	218 900	227 400	2.75

[a] All the experiments used KPS (1:5[RAFT]) as initiator, and all the initial aqueous pH values were about 2.80 without neutralization. The reaction temperature was kept at 70 °C. Post addition of NaOH solution technology was used to increase the colloidal stability. The emulsions have negligible amount of coagulum. The final solid content was about 30 wt %. [b] The digital numbers in the sample names represent the designed molecular weight of triblock copolymer. [c] The $M_{n,PSt-PnBA-PSt}$ was calculated from the GPC $M_{n,exp}$ data in the following rows. [d] The monomer conversion was measured by gravimetry. [e] The theoretical $M_{n,th}$ values were calculated from $M_{n,th} = M_{n,RAFT} + M_{monomer} x[M]/[RAFT]$, where [M] and [RAFT] represent the monomer and macroRAFT agent concentrations, and x is the conversion.

Table 2. Dead Chain fractions of PSt−PnBA−PSt Triblock Copolymer in Emulsion Polymerization Mediated by $PAA_{28}-PSt_5$ MacroRAFT Agent

		dead chain percentage[a]				
exp	sample	polystyrene (mol %)	PSt−PnBA (mol %)	PSt−PnBA−PSt (mol %)	total (mol %)	$n_{\text{diblock,max}}$ (mol %)[b]
1	30K−25K−30K	1.9	2.1	1.4	5.4	4.3
2	30K−55K−30K	1.9	2.4	1.4	5.7	5.1
3	30K−70K−30K	1.9	2.6	1.0	5.5	5.4
4	30K−90K−30K	2.0	3.0	0.9	5.9	6.4
5	30K−110K−30K	2.0	2.9	0.9	5.8	6.0
6	30K−140K−30K	2.0	3.2	0.9	6.1	6.7
7	30K−240K−30K	2.0	3.2	0.8	6.0	6.7
8	15K−90K−15K	1.6	3.4	1.0	6.0	7.0
9	45K−90K−45K	2.5	2.5	1.0	6.0	5.3
10	15K−45K−15K	1.6	2.9	1.0	5.5	6.0
11	45K−135K−45K	2.5	2.9	0.8	6.2	6.2

[a] The dead chain fractions in mole percentage were calculated by

$$n_D = 1 - \frac{[\text{RAFT}]_0}{[\text{RAFT}]_0 + af[\text{KPS}]_0(1 - e^{-k_d t})}$$

in which $[\text{RAFT}]_0$ and $[\text{KPS}]_0$ are the initial concentrations of macroRAFT agent and initiator KPS, f is the initiator efficiency factor, t is the polymerization time, and k_d is the dissociation rate constant of KPS, $a = 1$ for combination and 2 for disproportionation termination. Here we assumed that the termination mode occurred in our systems was combination, so $a = 1$. The values of k_d referred to ref 61 and f to ref 62. [b] The content of PSt−PnBA diblock was estimated by

$$n_{\text{diblock}} = \frac{bf[\text{KPS}]_0(e^{-k_d t_1} - e^{-k_d t_2})}{[\text{RAFT}]_0 + bf[\text{KPS}]_0(e^{-k_d t_1} - e^{-k_d t_2})}$$

in which t_1 and t_2 are reaction times from the beginning to the end of the chain extension of PnBA block. Let $b = 2$; one can obtain the maximum amount of PSt−PnBA diblock by assuming that all new-born polymer chains derived from the primary radical by KPS decomposition lead to the diblock copolymer.

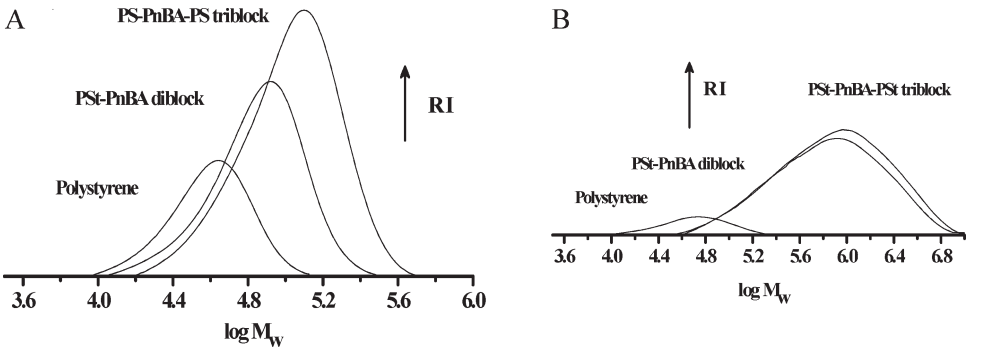

Figure 1. GPC chromatogram variations of before and after chain extensions during the synthesis of polystyrene-*b*-poly(*n*-butyl acrylate)-*b*-polystyrene (PSt−PnBA−PSt) triblock copolymer. Key: (A) 30K−25K−30K (experiment 1); (B) 30K−240K−30K (experiment 7). The digital numbers in the sample name represented the designed molecular weight of each block. [KPS]:[RAFT] = 1:5, the reaction temperature was 70 °C, and the final solid content was 30%.

polymerization, the M_n of PSt block was set to 30 kg/mol in this work. On the other hand, experiments 4, 8, and 9 were designed to have the same M_n of PnBA block (ca. 90 kg/mol) but different PSt M_n's from 15 to 45 kg/mol. This is to study possible influence of the PSt block molecular weight and its relatively broad distribution. Experiments 4, 10, and 11 formed the set of PSt−PnBA−PSt triblock copolymers that have different M_n's (from 15K−45K−15K to 45K−135K−45K) but the same copolymer composition (40 wt % PSt).

The PSt−PnBA−PSt triblock copolymer samples were synthesized by sequential addition of monomers. At each stage, monomer conversion was higher than 90%, as summarized in Table 1. The polymerization proceeded rapidly and the triblock copolymers were obtained within 4 h. All the emulsions had good colloidal stability with negligible amount of coagulum. The experimental molecular weights were in good agreement with the theoretical values even in the case of very high molecular weight (eg, 338 kg/mol in experiment 7.). The PDI's of experiments1 and 2 were relatively low but the others were high, which will be discussed.

The dead chain fractions in the PSt−PnBA−PSt samples were calculated and listed in Table 2. Owing to the very high polymerization rate resulted from a radical segregation effect,[19−25] the dead chain fractions were all lower than 6.2 mol %. The maximum levels of the diblock copolymer were also estimated and listed in Table 2. From Table 2, it is clear that the levels of the diblock copolymer in the final triblock copolymer, which could significantly deteriorate triblock copolymer performance,[18] were actually insignificant.

To elucidate formation of the triblock copolymer chains, GPC curves and particle numbers at the end of each stage in experiments 1 and 7 were monitored. The GPC curves are shown in Figure 1. All the GPC peaks in both experiments were unimodal. In experiment 1, the molecular weight increased from the first stage to the third stage and the polydispersity remained relatively low (e.g., PDI ~ 1.41 for PSt−PnBA−PSt triblock). In experiment 7, the molecular weight increased from the first stage to the second stage but the PDI increased significantly from 1.42 (PSt) to 3.02 (PSt−PnBA diblock). From the second stage to the third stage, the shift of

Table 3. Diameter and Number of Particles in Emulsion Polymerization Mediated by PAA_{28}-PSt_5 MacroRAFT Agent

		Polystyrene		PSt−PnBA		PSt−PnBA−PSt	
exp	sample	diameter (nm) (poly)[a]	N_p[b] (10^{16}/L)	diameter (nm) (poly) [a]	N_p[b] (10^{16}/L)	diameter (nm) (poly) [a]	N_p[b] (10^{16}/L)
1	30K−25K−30K	64 (0.03)	4.86	80 (0.03)	4.62	95 (0.04)	4.25
7	30K−240K−30K	50 (0.05)	2.91	107 (0.02)	2.67	117 (0.03)	2.27

[a] The particle diameter was measured by DLS. The distributions were all unimodal. [b] The number of particles N_p was calculated by $N_p = \frac{6m}{\pi D_v^3 d_p}$, in which m is the polymer mass in gram (g_{latex}^{-1}), d_p is the polymer density, 1.05 g·cm^{-3}, and D_v is the volume-average particle diameter measured by Malvern. Poly is the dispersity factor from Malvern, the lower the poly, the narrower the particle size distribution.

Table 4. Synthesis of PnBA, Poly(styrene-*co*-*n*-butyl acrylate) and Poly(styrene-*block*-*n*-butyl acrylate) (ie. PSt−PnBA) via Emulsion Polymerization Mediated by PAA_{28}-PSt_5 MacroRAFT Agent

exp[a]	polymer	convn[b] (%)	t (min)	$M_{n,th}$[c] (g/mol)	$M_{n,exp}$ (g/mol)	PDI	dead chain percentage [d] (mol %)
12	PnBA	98	120	149 500	157 900	1.44	4.6
13[e]	poly(St-*co*-nBA)	99	230	151 700	159 200	1.50	6.1
14[f]	PSt−PnBA	91	170	138 000	139 300	2.17	5.4

[a] All the experiments used KPS (1:5[RAFT]) as initiator, and the initial aqueous pH values were about 2.80 without neutralization. The reaction temperature was kept at 70 °C. The emulsions had negligible amount of coagulum at complete conversions. The final solid contents were about 30%. The polymerization involved two steps: First, a seeded emulsion with M_n 30 000 g/mol was synthesized via ab initio emulsion polymerization mediated by macroRAFT. Second, NaOH solution was injected to increase the colloidal stability and the second monomer (nBA in experiments 12 and 14; styrene and nBA mixture in experiment 13) was added at a rate of 20 g/h. [b] The monomer conversion was measured by gravimetry. [c] The theoretical Mn values were calculated from $M_{n,th} = M_{n,RAFT} + M_{monomer}x$[M]/[RAFT], where [M] and [RAFT] represent the monomer and macroRAFT agent concentrations, and x is the conversion. [d] The dead chain percentage was calculated by the same method as in Table 2. [e] The styrene content was 20 wt % in experiment 13. [f] The styrene content in experiment 14 was also 20 wt %.

the lower molecular weight portion of the curve appeared to be undetectable. It was likely that only a small fraction of chain length grew during this period of time, considering that the fraction of dead chains was very small, as seen in Table 2. Table 3 summarizes the data of particle diameter and number (N_p) of experiments 1 and 7 at each stage. In both cases, N_p decreased slightly in the second and third stages, likely due to limited coagulation. The particle size distributions at the different stages are narrow. It is evident that no second nucleation occurred in the second and third stages. It can thus be concluded that the dramatic increase in PDI at the second stage of experiment 7 was not caused by the second nucleation.

The PDIs of experiment 1 and experiment 2 triblock samples were relatively low, compared to experiments 3−11. The PDI values of experiments 1 and 2 were 1.37 and 1.46, it increased slightly to 1.64 in experiment 3 and dramatically to above 1.96 in experiments 4−11. The increase occurred mainly during the second stage in synthesizing PSt−PnBA diblock. The possible reasons for this molecular weight distribution broadening are as follows: (1) formation of dead chains, (2) new-born particles from the second nucleation, (3) diffusion-controlled RAFT addition due to increased molecular weight or gel effect that led to decrease in C_{tr},[63] (4) branching via radical transfer to PnBA,[64,65] and (5) influence of possible microphase separation inside particles. Reasons 1 and 2 have been excluded previously.

To find out the very reason for the PDI increase, three more experiments were designed as shown in Table 4. Experiment 12 was the RAFT emulsion polymerization of *n*-butyl acrylate. The final M_n was as high as 158 kg/mol and the PDI remained to be low at 1.44, suggesting that neither (3) diffusion-controlled RAFT addition caused by gel effect nor (4) branching via radical transfer to PnBA was responsible for the increased PDI. The copolymer compositions in experiments 13 and 14 were designed to be the same. Experiment 13 yielded a random copolymer having the final M_n 159 kg/mol, in agreement with its theoretical value. The PDI was also relatively low, at 1.50. In contrast, experiment 14 yielded a product having PDI 2.17, though its M_n's matched well with the theoretical values, as shown in Figure 2. The trend of the GPC traces during the polymerization of

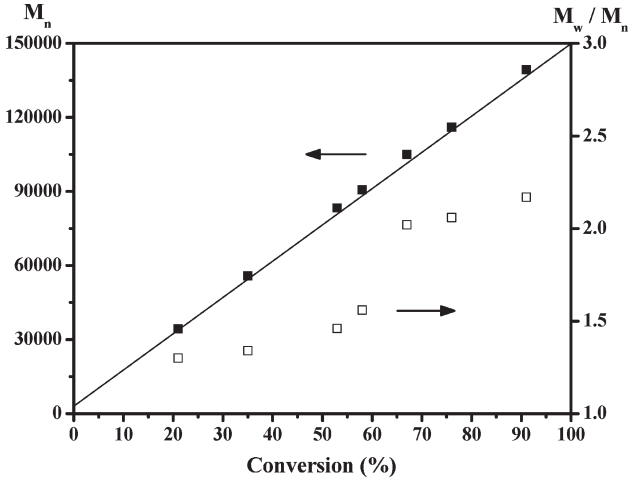

Figure 2. M_n (relative to polystyrene narrow standards) and PDI variation with the total conversions of styrene and *n*-butyl acrylate during the synthesis of polystyrene$_{30K}$-*b*-poly(*n*-butyl acrylate)$_{120K}$ (experiment 14). The line is the theoretical M_n. [KPS]:[RAFT] = 1:5, the final solid content is 30%, and the reaction temperature is 70 °C.

experiment 14 is shown in Figure 3. Before the M_n of PSt−PnBA diblock reached 105 kg/mol, the GPC curve gradually shifted forward to the high molecular weight end as the PnBA block length increased. When the diblock M_n was over 105 kg/mol, the part of low M_n species stopped increasing. Accordingly, before the conversion reached 58% (where the diblock M_n was 91 kg/mol), the PDI increased steadily and reached 1.56. After that, the PDI increased rapidly and reached 2.17 at the complete conversion. The distribution of trithiocarbonate RAFT groups in terms of molecular weight was detected by the GPC UV detector at 311 nm.[33,66] Figure 4 compares the RI and UV signals in the GPC measurement for the sample of M_n = 116K. The two curves are almost overlapped, revealing that majority of the polymer chains were still end-capped with the RAFT groups. Figure 5 shows the PDI versus PnBA composition. The PDI value increased dramatically for the PnBA compositions over 60 wt %. Similar trends were also observed in experiments 1−11, as shown in Table 1. The PnBA contents of experiments 1 and 2

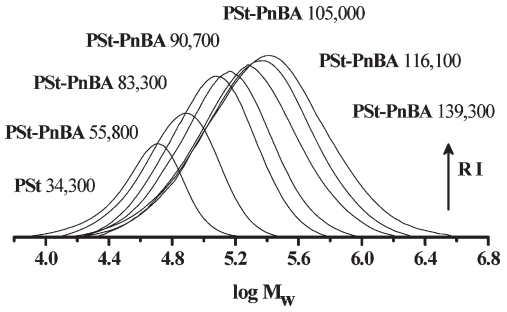

Figure 3. GPC chromatogram variations during the synthesis of polystyrene$_{30K}$-*b*-poly(*n*-butyl acrylate)$_{120K}$ (experiment 14). [KPS]:[RAFT] = 1:5, the final solid content is 30%, and the reaction temperature is 70 °C.

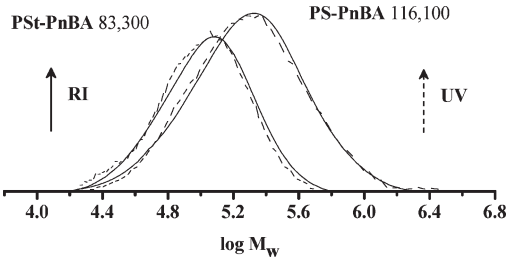

Figure 4. Comparison of GPC RI (solid lines) and UV 311 (dash lines) chromatograms during the synthesis of polystyrene$_{30K}$-*b*-poly(*n*-butyl acrylate)$_{120K}$ (experiment 14). [KPS]:[RAFT] = 1:5, final solid content is 30%, and reaction temperature is 70 °C.

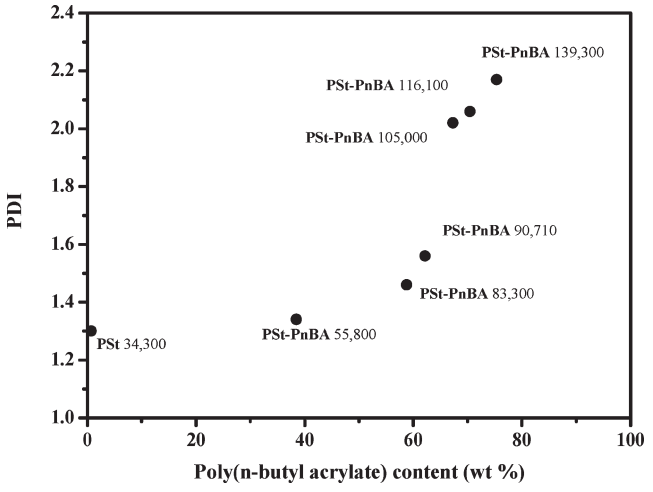

Figure 5. PDI versus poly(*n*-butyl acrylate) content during the synthesis of polystyrene$_{30K}$-*b*-poly(*n*-butyl acrylate)$_{120K}$ (experiment 14). The PnBA content was calculated by $\text{cont}_{\text{PnBA}} = [M_{\text{n,PSt-}b\text{-PnBA}} - M_{\text{n,PSt}}/M_{\text{n,PSt-}b\text{-PnBA}}$. [KPS]:[RAFT] = 1:5, final solid content 30%, and reaction temperature 70 °C.

samples were respectively 40.2 wt % and 59.6 wt %, with relatively low PDIs. The PnBA compositions of experiments 3−11 samples were all above 60 wt % with high PDIs.

Figure 6 shows the TEM micrographs of the particles obtained during the period of increasing PDI. The four samples between PSt−PnBA 55 800 to 105 000 in Figure 3 all showed two distinct glass transition temperatures (T_g) in the DSC measurement with −45 °C for PnBA block and 90 °C for PSt block, suggesting that there were microphase separations inside the particles. However, the particles appeared to be round, clear and homogeneous at the first as shown in Figure 6A. It is possible that PnBA domains were too small to be seen in the very beginning of phase separation. Some of them became blurring later, seen in Figure 6B.

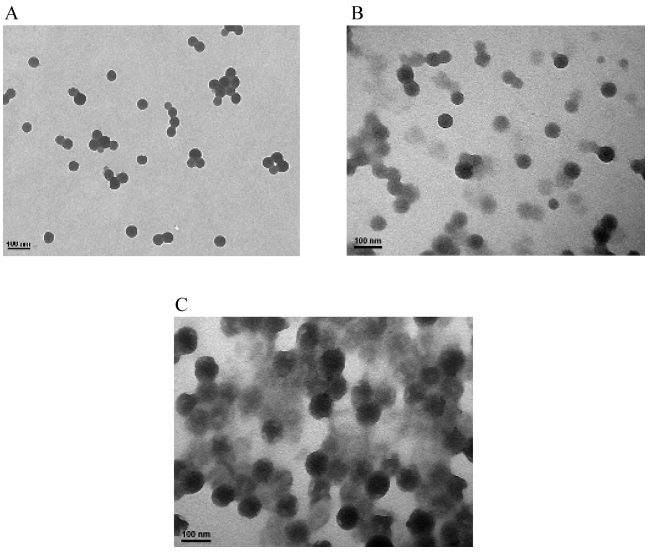

Figure 6. TEM micrographs of particles at various PnBA contents during the synthesis of polystyrene$_{30K}$-*b*-poly(*n*-butyl acrylate)$_{120K}$ (experiment 14). Polystyrene blocks were selectively stained by RuO_4. Key: (A) 58.8 wt % with PDI 1.46; (B) 62.1 wt % with PDI 1.56; (C) 67.3 wt % with PDI 2.02.

Finally, some bright inclusions (PnBA) were clearly visible at the particle surfaces in Figure 6C. In the Figure 6A sample, PSt was the continuous phase and thus the particles were round due to the high T_g of PSt. The Figure 6B sample experienced deformation in shape and became blurring because of the soft PnBA. However, due to the PAA segments that were covalently bonded to the PSt blocks and acted as stabilizer in the emulsion polymerization, the PSt domains resided at the particle surfaces, as seen in Figure 6C.

From the above results, it is evident that the jump in PDI was caused by the phase separation inside particles in experiments 1−11 and 14. It is well accepted that the viscosity of block copolymer is much higher than that of homogeneous polymer.[67] When the microphase separation occurred, the viscosity of the system would increase much. The mobility of the polymer chains could dramatically reduce so that the RAFT addition reaction could become diffusion-controlled.[63] In such a case, the transfer constant of the polymeric RAFT agent might decrease, resulting in the increase of PDI.

Phase Separation of PSt−PnBA−PSt Triblock Copolymer. The morphologies of the PSt−PnBA−PSt triblock samples were studied by TEM. However, the clear microphase separation could be observed only in the triblock copolymer of 45K−90K−45K, very likely due to the weak contrast. In Figure 7, the lamellae structure is clearly seen for the triblock copolymer of 45K−90K−45K.

Figure 8 summarizes DSC curves of all the samples. There were two T_g's (−45 °C for the PnBA block and 90 °C for the PSt block) except for the 30K−140K−30K, 30K−240K−30K, and 15K−90K−15K samples, in which the T_g of PSt was not detected probably due to their low PSt compositions. Dynamic mechanical analysis (DMA) is considered to be more sensitive in detecting T_g than DSC. Unfortunately, these samples were too soft to be analyzed by DMA.

Mechanical Properties of PSt−PnBA−PSt Triblock Copolymers. Figure 9 compares the stress−strain curves for the PSt−PnBA−PSt triblock copolymers having different PnBA molecular weights with the PSt molecular weight fixed at 30 kg/mol. All the samples except for 30K−25K−30K showed a typical triblock thermoplastic elastomer behavior: linear

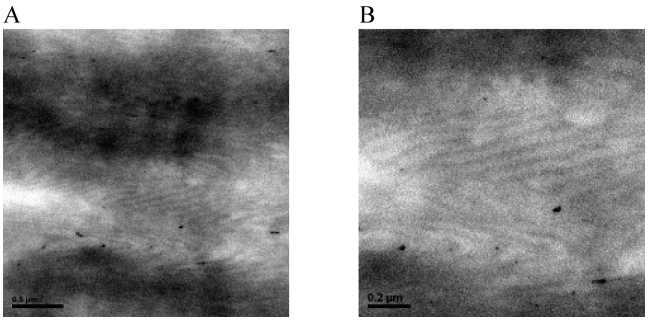

Figure 7. TEM micrographs for microphase separation of PSt−PnBA−PSt triblock copolymer polystyrene$_{45K}$-*b*-poly(*n*-butyl acrylate)$_{90K}$-*b*-polystyrene$_{45K}$ cast from THF and PSt block selective stained by RuO_4. The scale bar is 500 nm in A and 200 nm in B.

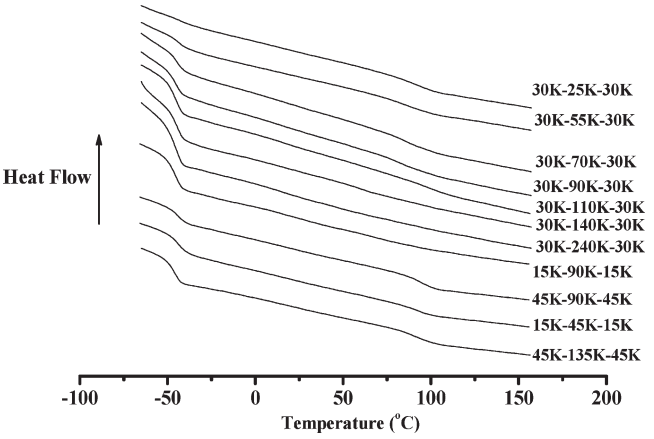

Figure 8. DSC traces for PSt−PnBA−PSt triblock copolymers in Table 1. Heating rate: 10 °C/min. The digital numbers in the sample names which represent the designed molecular weight of each block are listed next to the curves.

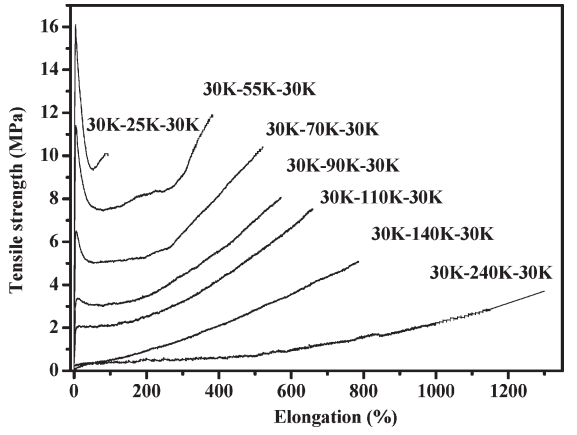

Figure 9. Effect of the PnBA block length on the stress−strain curve of PSt−PnBA−PSt triblock copolymers containing similar PSt block (about 30K g/mol) and cast from THF.

strain response followed by softening and then hardening. The 30K−25K−30K sample behaved more like a plastic, probably due to continuous PSt phase at this composition. Over a 12-fold elongation at break was observed with the sample having the highest PnBA molecular weight. The elastic modulus increased but the elongation at break reduced with decreasing the PnBA molecular weight, as it is the case for most TPEs.[60] Yielding occurred at low strain for the samples having relatively high PSt contents (above 40 wt %), due to a continuous PSt phase. The higher the PSt composition, the more pronounced the yielding was. At 71.5 wt % PSt (i.e., 30K−25K−30K), the yield stress exceeded the ultimate tensile strength.

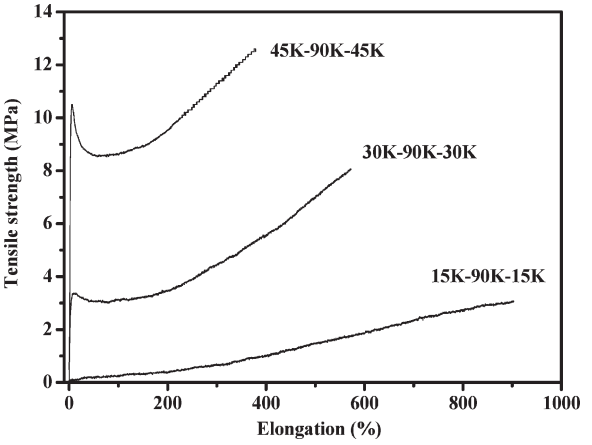

Figure 10. Effect of the PSt block length on the stress−strain curves for PSt−PnBA−PSt triblock copolymers containing similar PnBA block (about 90 kg/mol) and cast from THF.

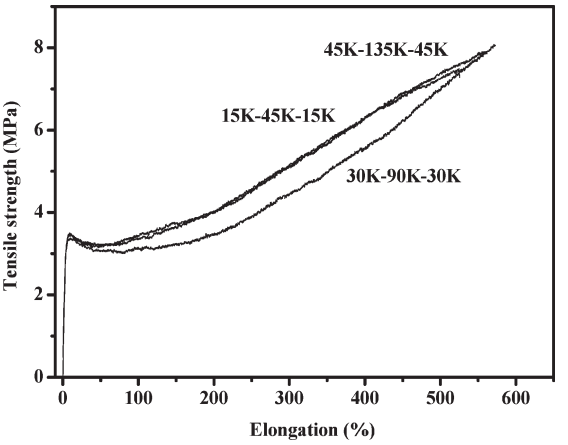

Figure 11. Effect of the triblock molecular weight on the stress−strain curves for PSt−PnBA−PSt triblock copolymers containing similar PSt content (about 40 wt %) and cast from THF.

Figure 10 shows the stress−strain curves of the second series of PSt−PnBA−PSt having different PSt but the same PnBA molecular weight (ie., 15K−90K−15K, 30K−90K−30K, and 45K−90K−45K in Table 1). An increase in the elastic modulus and a decrease in the elongation at break were observed as the PSt molecular weight was increased. This trend is expected for the increased "hard" composition.

For classic triblock copolymer thermoplastic elastomers such as SBS, the ultimate tensile strength is nearly independent of the "hard" block molecular weight if it is higher than the entanglement value (M_e) (10 kg/mol for PSt).[60] The ultimate tensile strength of SBS materials is independent of the composition when the PSt M_n is over 15 kg/mol until it forms the continuous PSt phase. Unexpectedly, the ultimate tensile strength of the current system increased with the PSt molecular weight. At the first thought, this could be ascribed to the relative high PSt block PDI.[12] However, when the PSt molecular weight was increased by increasing the total triblock copolymer molecular weight at similar compositions, the stress−strain curves overlapped, as seen in Figure 11. The PSt molecular weight had little influence on the PSt−PnBA−PSt mechanical properties. This is in sharp contrast to the data in Figure 10. It thus becomes clear that the relative high PDI of the PSt block was not the reason for the PSt

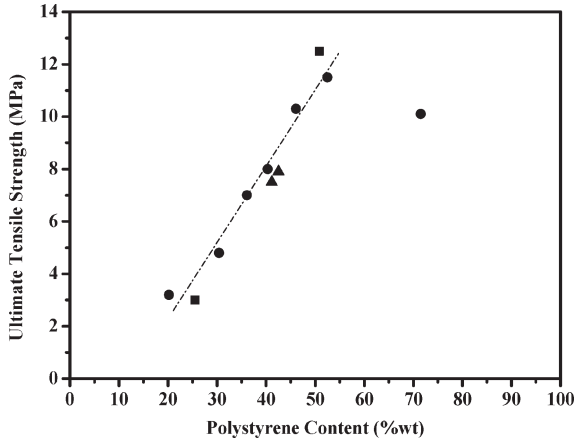

Figure 12. Ultimate tensile strength versus PSt content of PSt−PnBA−PSt triblock samples cast from THF in Table 5. Key: (●) 30K−25K−30K, 30K−55K−30K, 30K−70K−30K, 30K−90K−30K, 30K−110K−30K, 30K−140K−30K, and 30K−240K−30K. (■) 15K−90K−15K and 45K−90K−45K; (▲) exp 15K−45K−15K and 45K−135K−45K.

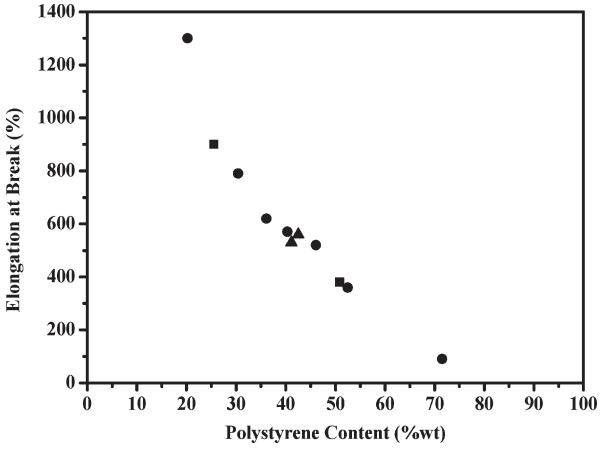

Figure 13. Elongation at break versus PSt content of PSt−PnBA−PSt triblock samples cast from THF in Table 5. Key: (●) 30K−25K−30K, 30K−55K−30K, 30K−70K−30K, 30K−90K−30K, 30K−110K−30K, 30K−140K−30K, and 30K−240K−30K; (■) 15K−90K−15K and 45K−90K−45K; (▲) exp 15K−45K−15K and 45K−135K−45K.

molecular weight dependence of the ultimate tensile strength as shown in Figure 10. In addition, the three triblock copolymers in Figure 11 had very different PDIs, also suggesting the insignificant effect of PDI on the tensile properties.

Figures 12−14 show the mechanical properties plotted against the copolymer composition for all the PSt−PnBA−PSt samples. The ultimate tensile strength linearly increased with the increased PSt composition when it was <52.5 wt %. The strength appeared to be a function of the composition only, independent of the molecular weight and PDI of each block. At 72.5 wt % PSt, the strength dropped for PSt formed a continuous phase. The reason for the linear strength-composition correlation for such a broad range remains to be elucidated.

The elongation at break increased as the decreased PSt composition, which is common with triblock TPEs.[60] A 13-fold elongation was reached at 20.2 wt % PSt. The elastic modulus remained at a low level with the PSt content ≤30.4 wt %, and increased significantly with further increase in the PSt content, as shown in Figure 14. The similar situation was reported for the PMMA−PnBA−PMMA triblock copolymers synthesized by anionic polymerization.[2]

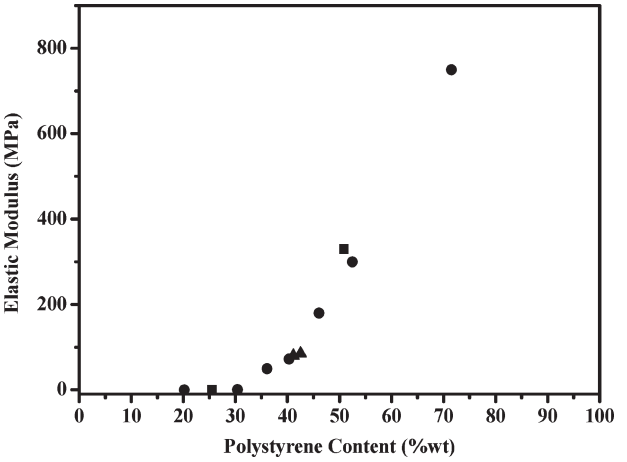

Figure 14. Elastic modulus versus PSt content of PSt−PnBA−PSt triblock samples cast from THF in Table 5. Key: (●) 30K−25K−30K, 30K−55K−30K, 30K−70K−30K, 30K−90K−30K, 30K−110K−30K, 30K−140K−30K, and 30K−240K−30K; (■) 15K−90K−15K and 45K−90K−45K; (▲) exp 15K−45K−15K and 45K−135K−45K.

As we discussed previously, the PDI increased sharply after nBA composition incorporated on the block copolymer higher than 60% during the polymer chain growth, as referred to Figure 4. This dramatic increase in PDI was ascribed to the decrease in the transfer coefficient of the polymeric RAFT agent. This leads to the concerns that some of diblock copolymer RAFT agents might not be effectively activated due to too low transfer coefficient during the third block extension of polystyrene. Interestingly, all the samples with largely varied PDI follow similar changing trend of the mechanical properties with the copolymer compositions as seen in Figures 12−14. Such a result indicates that most of the diblock copolymer might be activated in the third block extension to form triblock copolymer. As a matter of fact, when we largely changed the chain length of the third block polymer (polystyrene), we did not see the change in the mechanical properties of the triblock copolymer as seen in Figure 11. This suggests that the transfer coefficient should still be high enough to activate most of the diblock copolymer even in the case of the shortest chain length of the third block (15K), where the diblock copolymer could not be activated most likely. It will be interesting to see if the triblock copolymer of PSt−PnBA−PSt with very low PDI, which could be synthesized by the anionic polymerization, could be much superior to the current copolymer.

The mechanical properties of the triblock copolymer samples were summarized in Table 5. The highest ultimate tensile strength of the triblock copolymers is about 12 MPa. This value is still lower than the typical SBS (about 30 MPa in strength and 800−1000% elongation at break).[60] This could be attributed to the different entanglement molecular weights (M_e) for between PnBA and polybutadiene.[1] There are no reported mechanical properties of PSt−PnBA−PSt triblock synthesized by anionic polymerization for comparison. Jerome et al. studied the system of PMMA−PnBA−PMMA obtained through transesterification of the anionically synthesized PMMA-*b*-Poly(*tert*-butyl acrylate)-*b*-PMMA. The typical ultimate mechanical strength and elongation at break were 10−15 MPa and 700%, respectively.[2] Also for comparison, the highest strength and elongation of PMMA−PnBA−PMMA triblocks synthesized by bulk and solution ATRPs were reported to be 5.0 MPa and 385% at 31.4 wt % PMMA in ref 11 and 4.2 MPa and 415% at 26 wt % PMMA in ref 12, which were much lower than their anionic polymerization

Table 5. Mechanical Properties and Shore Hardness of PSt−PnBA−PSt Triblock Copolymers via Emulsion Polymerization Mediated by PAA_{28}-PSt_5 MacroRAFT agent

exp	sample[a]	polystyrene (wt %)[b]	ultimate tensile strength (MPa)	elongation at break (%)	elastic modulus (MPa)[c]	hardness (H_A)
1	30K−25K−30K	71.5	10.1	90	750	91
2	30K−55K−30K	52.5	11.5	360	300	90
3	30K−70K−30K	46.1	10.3	520	180	85
4	30K−90K−30K	40.3	8.0	570	72	83
5	30K−110K−30K	36.1	7.0	620	50	77
6	30K−140K−30K	30.4	4.8	790	0.8	38
7	30K−240K−30K	20.2	3.2	1300	0.22	17
8	15K−90K−15K	25.5	3.0	900	0.25	24
9	45K−90K−45K	50.8	12.5	380	330	88
10	15K−45K−15K	42.5	7.9	560	85	85
11	45K−135K−45K	41.1	7.5	530	80	81

[a] All the film samples were THF cast with three days casting followed by drying in vacuum at 120 °C for 24 h. [b] The PSt content was determined by ^{1}H NMR using $CDCl_3$ as solvent. [c] The elastic modulus (experiments 1−5 and experiments 9−11) was calculated from the stress−strain data at <10% low elongation. Experiments 6−8 samples were soft and their elastic modulus was calculated at 10% to 50% elongation.

counterparts, even though the ATRP triblock copolymers had PDI's as low as 1.18 and 1.15. The relatively high PDI in the PMMA block was blamed for the poor mechanical properties of the PMMA−PnBA−PMMA triblock samples. The highest mechanical properties of the current triblock copolymers are at higher composition of the "hard" block and are over two-folds of that of the bulk and solution.[11,12] The current strength is close to that of the anionic polymerization product but the elongation at break is not as good.[2] The Shore hardness of PSt−PnBA−PSt triblock copolymers could be tuned at a wide range (H_A 17−91) by changing the PSt content (20.2−71.5 wt %), as shown in Table 5.

Conclusions

A series of PSt−PnBA−PSt samples with designed chain structures were synthesized via an emulsion polymerization using amphiphilic co-oligomer macroRAFT agent as surfactant and chain transfer agent. The effect of chain structures on the mechanical properties of the triblock copolymer materials was investigated. The following conclusions are reached:

The triblock copolymers were prepared within four hours, having high monomer conversion and small amount of dead chains. During the synthesis of PS-PnBA diblock copolymers, the PDI increased dramatically when PnBA exceeded 60 wt %, probably due to a phase separation occurred inside particles.

The ultimate tensile strength was a function of the composition only and it unexpectedly increased linearly with the PSt composition up to about 50 wt %. The highest strength was about 12 MPa. The elongation at break increased as the PSt composition decreased. A 13-folds of elongation was obtained at 20.2 wt % PSt. The elastic modulus remained low at the PSt ≤ 30.4 wt %, and it then increased rapidly with the increase of PSt composition. The optimal mechanical properties of PSt−PnBA−PSt, that compromised strength and elongation were 10 MPa tensile strength and 500% elongation at break, which were obtained between 40−50 wt % PSt. This work, for the first time, demonstrated that the RAFT emulsion polymerization holds good promise for synthesis of thermoplastic elastomer materials.

Acknowledgment. The authors would like to thank the National Science Foundation of China (NSFC) for Award No. 20836007 for supporting this research.

References and Notes

(1) Tong, J. D.; Jerome, R. *Macromolecules* **2000**, *33*, 1479–1481.
(2) Tong, J. D.; Jerome, R. *Polymer* **2000**, *41*, 2499–2510.
(3) Tong, J. D.; Leclere, Ph.; Doneux, C.; Bredas, J. L.; Lazzaroni, R.; Jerome, R. *Polymer* **2001**, *42*, 3503–3514.
(4) Zetterlund, P. B.; Kagawa, Y.; Okubo, M. *Chem. Rev.* **2008**, *108*, 3747–3794.
(5) Hawker, C. J.; Bosman, A. W.; Harth, E. *Chem. Rev.* **2001**, *101*, 3661–3688.
(6) Matyjaszewski, K.; Xia, J. *Chem. Rev.* **2001**, *101*, 2921–2990.
(7) Kamigaito, M.; Ando, T.; Sawamoto, M. *Chem. Rev.* **2001**, *101*, 3689–3745.
(8) Chiefari, J.; Chong, Y. K.; Ercole, F.; Krstina, J.; Jeffery, J.; Le, T. P. T.; Mayadunne, R. T. A.; Meijs, G. F.; Moad, C. L.; Moad, G.; Rizzardo, E.; Thang, S. H. *Macromolecules* **1998**, *31*, 5559–5562.
(9) Robin, S.; Guerret, O.; Couturier, J.; Pirri, R.; Gnanou, Y. *Macromolecules* **2002**, *35*, 3844–3848.
(10) Mayadunne, T. A. R.; Rizzardo, E.; Chiefari, J.; Krstina, J.; Moad, G.; Postma, A.; Thang, S. H. *Macromolecules* **2000**, *33*, 243–245.
(11) Moineau, C.; Minet, M.; Teyssie, P.; Jerome, R. *Macromolecules* **1999**, *32*, 8277–8282.
(12) Tong, J. D.; Moineau, G.; Leclere, Ph.; Bredas, J. L.; Lazzaroni, R.; Jerome, R. *Macromolecules* **2000**, *33*, 470–479.
(13) Moineau, G.; Minet, M.; Teyssie, P.; Jerome, R. *Macromol. Chem. Phys.* **2000**, *201*, 1108–1114.
(14) Davis, K. A.; Matyjaszewski, K. *Macromolecules* **2000**, *33*, 4039–4047.
(15) Davis, K. A.; Matyjaszewski, K. *Macromolecules* **2001**, *34*, 2101–2107.
(16) Huang, J.; Jia, S.; Siegwart, D. J.; Kowalewski, T.; Matyjaszewski, K. *Macromol. Chem. Phys.* **2006**, *207*, 801–811.
(17) Braunecker, W. A.; Matyjaszewski, K. *Prog. Polym. Sci.* **2007**, *32*, 93–146.
(18) Yu, J. M.; Dubois, Ph.; Teyssie, Ph.; Jerome, R. *Macromolecules* **1996**, *29*, 6090–6099.
(19) Butte, A.; Storti, G.; Morbidelli, M. *Macromolecules* **2001**, *34*, 5885–5896.
(20) Luo, Y.; Wang, R.; Yang, L; Yu, B.; Li, B.; Zhu, S. *Macromolecules* **2006**, *39*, 1328–1337.
(21) Zetterlund, P. B.; Okubo, M. *Macromolecules* **2006**, *39*, 8959–8967.
(22) Kagawa, Y.; Zetterlund, P. B.; Minami, H.; Okubo, M. *Macromol. Theory Simul.* **2006**, *15*, 608–613.
(23) Maehata, H.; Buragina, C.; Cunningham, M.; Keoshkerian, B. *Macromolecules* **2007**, *40*, 7126–7131.
(24) Delaittre, G.; Charleux, B. *Macromolecules* **2008**, *41*, 2361–2367.
(25) Simms, R. W.; Cunningham, M. F. *Macromolecules* **2008**, *41*, 5148–5155.
(26) Luo, Y.; Tsavalas, J.; Schork, F. J. *Macromolecules* **2001**, *34*, 5501–5507.
(27) Luo, Y.; Cui, X. *J. Polym. Sci., Part A: Polym. Chem.* **2006**, *44*, 2837–2847.
(28) Lansalot, M.; Davis, T. P.; Heuts, J. P. A. *Macromolecules* **2002**, *35*, 7582–7591.
(29) Barner-Kowollik, C.; Buback, M.; Charleux, B.; Coote, M. L.; Drache, M.; Fukuda, T.; Goto, A.; Klumperman, B.; Lowe, A. B.; McLeary, J. B.; Moad, G.; Monteiro, M. J.; Sanderson, R. D.; Tonge, M. P.; Vana, P. *J. Polym. Sci., Part A: Polym. Chem.* **2006**, *44*, 5809–5831.
(30) Wang, A. R.; Zhu, S.; Kwak, Y.; Goto, A.; Fukuda, T.; Monteiro, M. J. *J. Polym. Sci., Part A: Polym. Chem.* **2003**, *41*, 2833–2839.
(31) Barner-Kowollik, C.; Coote, M. L.; Davis, T. P.; Radom, L.; Vana, P. *J. Polym. Sci., Part A: Polym. Chem.* **2003**, *41*, 2828–2832.
(32) Russum, J. P.; Jones, C. W.; Schork, F. J. *Macromol. Rapid Commun.* **2004**, *25*, 1064–1068.

(33) Smulders, W. W.; Jones, C. W.; Schork, F. J. *Macromolecules* **2004**, *37*, 9345–9354.
(34) Tsavalas, J. G.; Schork, F. J.; de-Brouwer, H.; Monteiro, M. J. *Macromolecules* **2001**, *34*, 3938–3946.
(35) de-Brouwer, H.; Monteiro, M. J.; Tsavalas, J. G.; Schork, F. J. *Macromolecules* **2000**, *33*, 9239–9246.
(36) Moad, G.; Chiefari, J.; Chong, Y. K.; Krstina, J.; Mayadunne, R. T. A.; Postma, A.; Rizzardo, E.; Thang, S. H. *Polym. Int.* **2000**, *49*, 993–1001.
(37) Yang, L.; Luo, Y.; Li, B. *J. Polym. Sci., Part A: Polym. Chem.* **2005**, *43*, 4972–4979.
(38) Bowes, A.; McLeary, J. B.; Sanderson, R. D. *J. Polym. Sci., Part A: Polym. Chem.* **2007**, *45*, 588–604.
(39) Matahwa, H.; McLeary, J. B.; Sanderson, R. D. *J. Polym. Sci., Part A: Polym. Chem.* **2006**, *44*, 427–442.
(40) McLeary, J. B.; Tonge, M. P.; de Wet Roos, D.; Sanderson, R. D.; Klumperman, B. *J. Polym. Sci., Part A: Polym. Chem.* **2004**, *42*, 960–974.
(41) Luo, Y.; Liu, X. *J. Polym. Sci., Part A: Polym. Chem.* **2004**, *42*, 6248–6258.
(42) Yang, L.; Luo, Y.; Li, B. *Polymer* **2006**, *47*, 751–762.
(43) Yang, L.; Luo, Y.; Li, B. *J. Polym. Sci., Part A: Polym. Chem.* **2006**, *44*, 2293–2306.
(44) Luo, Y.; Liu, B.; Wang, Z.; Gao, J.; Li, B. *J. Polym. Sci., Part A: Polym. Chem.* **2007**, *45*, 2304–2315.
(45) Shim, S. E.; Lee, H.; Choe, S. *Macromolecules* **2004**, *37*, 5565–5571.
(46) Russum, J. P.; Barbre, N. D.; Jones, C. W.; Schork, F. J. *J. Polym. Sci., Part A: Polym. Chem.* **2005**, *43*, 2188–2193.
(47) Simms, R. W.; Davis, T. P.; Cunningham, M. F. *Macromol. Rapid Commun.* **2005**, *26*, 592–595.
(48) Ferguson, C. J.; Hughes, R. J.; Pham, B. T. T.; Hawkett, B. S.; Gilbert, R. G.; Serelis, A. K.; Such, C. H. *Macromolecules* **2002**, *35*, 9243–9245.
(49) Ferguson, C. J.; Hughes, R. J.; Nguyen, D.; Pham, B. T. T.; Gilbert, R. G.; Serelis, A. K.; Such, C. H.; Hawkett, B. S. *Macromolecules* **2005**, *38*, 2191–2204.
(50) Ganeva, D. E.; Sprong, E.; de Bruyn, H.; Warr, G. G.; Such, C. H.; Hawkett, B. S. *Macromolecules* **2007**, *40*, 6181–6189.
(51) Rieger, J.; Stoffelbach, F.; Bui, C.; Alaimo, D.; Jerome, C.; Charleux, B. *Macromolecules* **2008**, *41*, 4065–4068.
(52) Rieger, J.; Osterwinter, G.; Bui, C.; Stoffelbach, F.; Charleux, B. *Macromolecules* **2009**, *42*, 5518–5525.
(53) Urbani, C. N.; Monteiro, M. J. *Aust. J. Chem.* **2009**, *62*, 1528–1532.
(54) Nicolas, J.; Charleux, B.; Guerret, O.; Magnet, S. *Angew. Chem., Int. Ed.* **2004**, *43*, 6186–6189.
(55) Nicolas, J.; Charleux, B.; Guerret, O.; Magnet, S. *Macromolecules* **2005**, *38*, 9963–9973.
(56) Nicolas, J.; Charleux, B.; Magnet, S. *J. Polym. Sci., Part A: Polym. Chem.* **2006**, *44*, 4142–4153.
(57) Wang, X.; Luo, Y.; Li, B.; Zhu, S. *Macromolecules* **2009**, *42*, 6414–6421.
(58) Barner-Kowollik, C.; Heuts, J. P. A.; Davis, T. P. *J. Polym. Sci., Part A: Polym. Chem.* **2001**, *39*, 656–664.
(59) Ferguson, C. J.; Russell, G. T.; Gilbert, R. G. *Polymer* **2002**, *43*, 6371–6382.
(60) *Thermoplastic elastomers*; Holden, G.; Legge, N. R.; Quirk, R.; Schroeder, H. E., 2nd ed.; Hanser: Munich, Germany, Vienna, and New York, 1996.
(61) Santos, A. M.; Vindevoghel, P.; Graillat, C.; Guyot, A.; Guillot, J. *J. Polym. Sci., Part A: Polym. Chem.* **1996**, *34*, 1271–1281.
(62) Gilbert, R. G. *Emulsion Polymerization: A Mechanistic Approach*; Academic Press: London, 1995.
(63) Yang, L.; Luo, Y.; Liu, X.; Li, B. *Polymer* **2009**, *50*, 4334–4342.
(64) Ahmad, N. M.; Heatley, F.; Lovell, P. A. *Macromolecules* **1998**, *31*, 2822–2827.
(65) Plessis, C.; Arzamendi, G.; Leiza, J. R.; Schoonbrood, H. A. S.; Charmot, D.; Asua, J. M. *Macromolecules* **2000**, *33*, 4–7.
(66) Baussard, J. F.; Habib-Jiwan, J. L.; Laschewsky, A.; Mertoglu, M.; Storsberg, J. *Polymer* **2004**, *45*, 3615–3626.
(67) Potschke, P.; Paul, D. R. *J. Polym. Sci., Part C: Polym. Rev.* **2003**, *43*, 87–141.